Plant Physiol. (1987) 84, 526–534
0032-0889/87/84/0526/09/$01.00/0

Variable Effects of Nitrate on ATP-Dependent Proton Transport by Barley Root Membranes

Received for publication October 17, 1986 and in revised form February 3, 1987

FRANCES M. DUPONT
United States Department of Agriculture, Agricultural Research Service, Westen Regional Research Center, Albany, California 94710

ABSTRACT

The effects of NO_3^- and assay temperature on proton translocating ATPases in membranes of barley (*Hordeum vulgare* L. cv California Mariout 72) roots were examined. The membranes were fractionated on continuous and discontinuous sucrose gradients and proton transport was assayed by monitoring the fluorescence of acridine orange. A peak of H^+-ATPase at 1.11 grams per cubic centimeter was inhibited by 50 millimolar KNO_3 when assayed at 24°C or above and was tentatively identified as the tonoplast H^+-ATPase. A smaller peak of H^+-ATPase at 1.16 grams per cubic centimeter, which was not inhibited by KNO_3 and was partially inhibited by vanadate, was tentatively identified as the plasma membrane H^+-ATPase. A step gradient gave three fractions enriched, respectively, in endoplasmic reticulum, tonoplast ATPase, and plasma membrane ATPase. There was a delay before 50 millimolar KNO_3 inhibited ATP hydrolysis by the tonoplast ATPase at 12°C and the initial rate of proton transport was stimulated by 50 millimolar KNO_3. The time course for fluorescence quench indicated that addition of ATP in the presence of KNO_3 caused a pH gradient to form that subsequently collapsed. This biphasic time course for proton transport in the presence of KNO_3 was explained by the temperature-dependent delay of the inhibition by KNO_3. The plasma membrane H^+-ATPase maintained a pH gradient in the presence of KNO_3 for up to 30 minutes at 24°C.

The characteristic that is used most frequently to identify the tonoplast ATPase is that the enzyme is inhibited by NO_3^- but not by vanadate or azide (3, 5, 9, 19–21, 24, 26, 31). Other inhibitors of the tonoplast ATPase, such as DCCD, are less useful, because they affect all of the proton-translocating ATPases (31). However, the effects of NO_3^- on the tonoplast H^+-ATPase are complex (4, 18) and NO_3^- inhibits other ATPases as well. For example, a putative Golgi membrane H^+-ATPase was partially inhibited by NO_3^- (7) and the mitochondrial F_1F_0-ATPase was inhibited by NO_3^- (27, 31). It is important to clarify the effects of nitrate on the tonoplast ATPase for several reasons. The criteria for using NO_3^- to identify the tonoplast ATPase need to be defined, particularly since there is some confusion in the literature between the effects of NO_3^- as an inhibitor of the ATPase and as a substrate for a NO_3^-/H^+ symport (4). The effect of NO_3^- on the tonoplast ATPase *in vivo* also needs to be elucidated. The physiological significance of the NO_3^--inhibition is unclear and puzzling, because the vacuole stores nitrate (23, 29). Nitrate inhibits the mitochondrial F_1F_0-ATPase and the tonoplast H^+-ATPase with a K_i of only 5 to 10 mM (27, 31) although it was estimated that the cytoplasmic concentration of nitrate was approximately 4 mM and the vacuolar concentration was greater than 40 mM for barley leaf protoplasts (23).

Barley roots have been used extensively for studies of ion transport and nitrogen metabolism, but until recently it has been difficult to obtain membrane preparations from barley that are suitable for studies of ion transport *in vitro*. In a previous paper (12) we described a method for separating barley membranes on sucrose gradients. The present paper describes the use of linear and discontinuous sucrose gradients to separate and characterize the proton-translocating ATPases from barley roots. The effects of nitrate and assay temperature on the proton-translocating ATPases were examined. Assays of transport at low temperatures emphasized the complex effects of nitrate on the tonoplast H^+-ATPase.

MATERIALS AND METHODS

Plant Material. Seeds of barley (*Hordeum vulgare* L. cv California Mariout 72) were grown as previously described (12) above an aerated solution containing either 0.1 mM $CaSO_4$ or full strength nutrients (13), with NH_4^+ as the sole source of nitrogen, unless otherwise indicated. Seedlings were maintained at 22°C for 7 d (22° roots) or at 22°C for 4 d, then transferred to 8 or 10°C for 6 d (8 or 10° roots). Each experiment described in this paper is a representative example of experiments that were performed on membranes from plants grown with several different growth regimes. In some cases, there appeared to be quantitative differences in the results. For example, there appeared to be a lower temperature optimum for proton transport for membranes from roots grown at lower temperatures (F DuPont, unpublished data). However, the basic pattern of the response to nitrate and temperature that is discussed in this paper was not affected by the growth regime and the different growth regimes did not alter the distribution of membranes on sucrose gradients.

Membrane Preparations. The procedures were modified from those of DuPont and Hurkman (12). The roots were excised, homogenized within 5 min of harvest, filtered through cheesecloth, centrifuged at 10,000*g* for 20 min in a Sorvall[1] GSA rotor, and the pellet discarded. The 10,000*g* supernatant was centrifuged at 100,000 rpm for 35 min in a Beckman 45 Ti rotor. The pellet was resuspended in 2 to 3 ml of suspension buffer consisting of 0.25 M sucrose and 2 mM DTT in 5 mM Pipes-KOH (pH 7.0), layered onto continuous (12) or discontinuous sucrose gradients, and centrifuged at 80,000*g* for 3 h. Two ml fractions were collected from the 15 to 45% (w/w) continuous gradients. The discontinuous gradients consisted of 14, 10, and 10 ml of 40, 30, and 22% (w/w) sucrose, respectively. The interfaces were collected from the step gradients by piercing the sides of the centrifuge tubes (Beckman Ultraclear tubes) with a syringe. Un-

[1] Mention of a specific product name by the United States Department of Agriculture does not constitute an endorsement and does not imply a recommendation over other suitable products.

less otherwise indicated, the interface samples were diluted with 250 mM KCl and 2 mM DTT in 25 mM Tris-HCl (pH 8.0) to a final concentration of 150 mM KCl and 15 mM Tris-HCl in a volume of 28 ml and then centrifuged at 100,000*g* for 35 min in a Beckman 42.1 rotor. The pellet was resuspended in suspension buffer and frozen at −70°C for up to 2 months. There was no noticeable difference in results for material frozen 1 d or 2 months.

Proton Transport Assays. ATP-dependent and PPi-dependent proton transport were assayed as the quenching of acridine orange fluorescence. A Farrand System 3 spectrofluorometer was equipped with a water jacketed cuvette holder. Temperature control was provided by a Neslab RTE-9DD circulating water bath. A constant stream of N_2 over the cuvette prevented condensation at low temperatures, and was used at all temperatures. Cuvette temperature was measured with a Fluke 2175A digital thermocouple thermometer. The assay solution, which was kept at the assay temperature, consisted of 2 μM acridine orange, 1 mM $MgSO_4$, and 0.25 M sucrose in 5 mM Pipes-KOH (pH 7.0), plus other salts as indicated. Pipes was chosen for the buffer because of the low temperature coefficient of the pK. An aliquot of assay solution was placed in a cuvette, the fluorescence intensity was monitored to assure temperature stability, an aliquot of membranes was then added, and transport was initiated within 1 min by addition of Na^+-ATP or Tris-ATP to a final concentration of 1 mM, or KPPi to a final concentration of 0.33 mM. The total volume was 3 ml. Fluorescence emission was measured at 528 nm (slit width 5 nm), using an excitation wavelength of 493 nm (slit width 2.5 nm). Solutions were mixed by drawing the sample up and down with a wide-bore plastic transfer pipette.

ATPase Assays. ATP hydrolysis was measured using the same assay solution as the fluorescence assays (12). ADPase and IDPase were assayed in a similar manner, using 1 mM ADP or IDP, 1 mM $MnCl_2$, 0.02% (v/v) Triton X-100 and 5 mM Pipes-KOH (pH 7.0). Assays were initiated by addition of membranes. Assays were carried out for 20 to 30 min at the indicated temperature and Pi determined by the method of Ames (2). For the time-course experiments, Pi was determined using the method of Sanui (30). The membranes were added, with mixing, to the assay solution in a conical centrifuge tube in a temperature controlled water bath. At timed intervals, 0.5 ml aliquots were removed and placed in 2.0 ml of 9% (w/v) TCA and 0.94% (w/v) ammonium molybdate in 0.75 M H_2SO_4. Within 20 min the Pi was extracted in 2.0 ml of butyl acetate, and within 2 h the Pi was determined by measuring the A_{310} of the butyl acetate.

Other Assays. NADH- and NADPH-Cyt *c* reductase, Cyt *c* oxidase, glucan synthase I and II, and protein assays were performed as described previously (11, 12), except 0.14 μCi of UDP-[U-^{14}C]glucose was used in the glucan synthase I and II assays. Sterol glycosyl transferase was assayed by the method of Hartmann-Bouillon and Benveniste (16), and also used 0.14 μCi of UDP-[U-^{14}C]glucose in each assay.

RESULTS

Proton Transport by Microsomal Membranes. Barley seedlings were grown at 10°C. A 10,000 to 100,000*g* membrane fraction was prepared and assayed for the effect of temperature and anions on ATP-dependent proton transport. When proton transport was assayed at 8, 16, and 24°C there was little transport when the impermeant sulfate anion was used (Fig. 1). Relatively high rates of transport were obtained over the 8 to 24°C temperature range when the assay mixture contained 50 mM KCl. In contrast, the effect of KNO_3 on proton transport was temperature dependent. In the presence of 50 mM KNO_3, at 24°C, there was a small initial quench of fluorescence when ATP was added, followed by a return of fluorescence to the original intensity. When the membranes were assayed at lower temperatures, the extent of

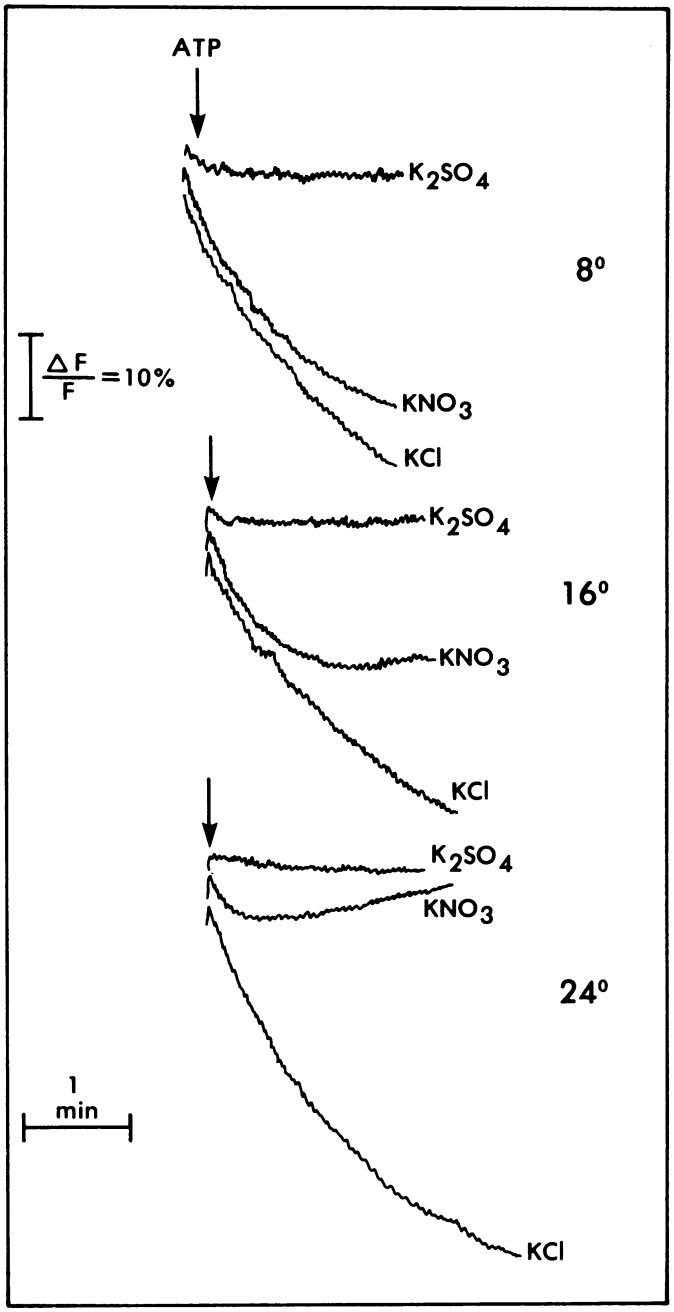

FIG. 1. Response of acridine orange fluorescence to addition of ATP. Membranes from the 10,000 to 100,000*g* pellet were assayed at the indicated temperatures with 50 mM KCl, 50 mM KNO_3, or 25 mM K_2SO_4. The initial fluorescence intensity for each trace is offset from the others so that the different traces can be distinguished. The membranes (64 μg protein per assay) were from barley roots grown in 0.1 mM $CaSO_4$ at 10°C.

transport in the presence of KNO_3 increased and the initial rate of transport was similar for KCl and KNO_3. The largest ΔpH[2] obtained in the presence of KNO_3 was at the lowest temperature measured. It was difficult to detect any transport in the presence of 50 mM KNO_3 at temperatures above 28°C (not shown). It was not possible to estimate the relative amounts of proton transport by the tonoplast ATPase in the microsomal fraction by calculating the percentage of transport that was inhibited by NO_3^-,

[2] Abbreviation: ΔpH, pH gradient.

because the effect of KNO_3 varied greatly, depending upon the assay temperature.

Continuous Sucrose Gradients. The membranes of the 10,000 to 100,000*g* pellets were separated on linear sucrose gradients and the fractions were assayed at 24°C for ATP-dependent proton transport in the presence of 50 mM KCl or 50 mM KNO_3 (Fig. 2). In the presence of KCl there was a broad peak of proton transport activity between 1.08 and 1.13 $g \cdot cm^{-3}$, with a maximum at 1.11 $g \cdot cm^{-3}$, and there was a shoulder of activity from 1.14 to 1.18 $g \cdot cm^{-3}$ (Fig. 2A). The activity of the peak at 1.11 $g \cdot cm^{-3}$ was almost entirely inhibited by KNO_3, and this is a density commonly reported for tonoplast vesicles (3, 19, 26, 31). For ease of discussion, this will be referred to as the tonoplast peak.

Two small peaks of proton transport activity apparently were not inhibited by nitrate, if only the initial rates were examined (Fig. 2A). However, the pattern of ATP-dependent proton transport for the two peaks was quite different. The first peak was in the tonoplast region of the gradient, at 1.12 $g \cdot cm^{-3}$, and the time course for fluorescence quench resembled that shown in Figure 1 for KNO_3 at 24°C. There was a small initial rate of quench, followed by a return of fluorescence to the original intensity (not shown). It was difficult to obtain an accurate estimate of initial rates in the presence of KNO_3 at 24°C, because it was necessary to decide whether to measure or to ignore the small downward slopes that were of short duration and were followed by an upward slope as in Figure 1. Also, a much smaller amount of protein was used per assay when assaying the gradient fractions than was used in Figure 1, further obscuring the biphasic time course. Therefore, the data for the tonoplast region of the gradient in Figure 2A are only a rough approximation of the true initial rates in the presence of KNO_3. The second peak of nitrate-insensitive ATPase was at a density of 1.14 to 1.18 $g \cdot cm^{-3}$ which is typical for plant plasma membranes (3, 10, 26, 31). The pattern of quench was similar in the presence of KCl or KNO_3, with no tendency of KNO_3 subsequently to dissipate the ΔpH (not shown), and the rates measured in the presence of KNO_3 were more accurate than in the tonoplast region of the gradient (Fig. 2A).

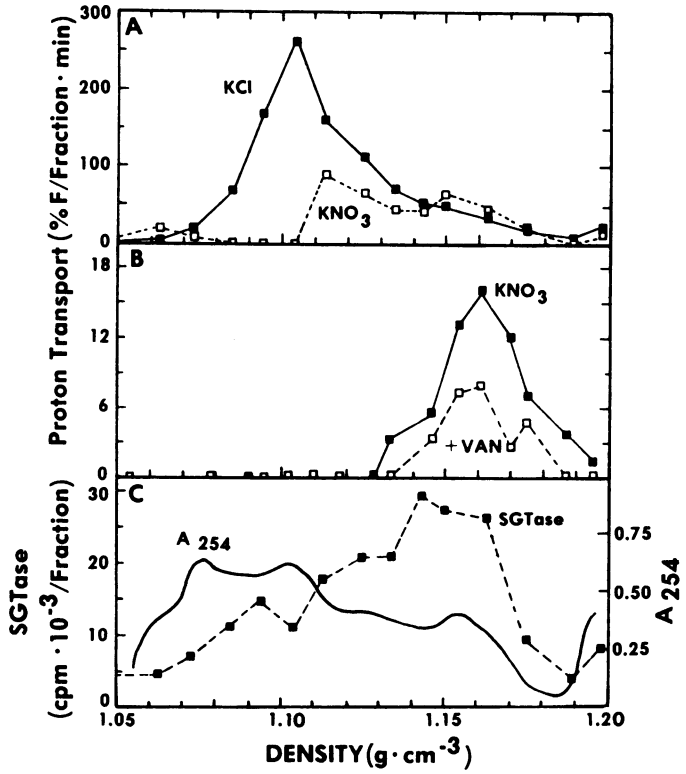

FIG. 2. Distribution of enzyme activities on a continuous sucrose gradient. A, Proton transport assayed with 50 mM KCl (■), or 50 mM KNO_3 (□). B, Proton transport assayed with 100 mM KNO_3 and 1 μM valinomycin (■); same, plus 300 μM sodium vanadate (□). C, Sterol glycosyl transferase (■), A_{254} (——). The membranes were from two separate experiments, and were from 19 g fresh weight for A and C, and 13 g fresh weight for B. All were from roots grown at 22°C in 0.1 mM $CaSO_4$. Assays were at 24°C.

Valinomycin had different effects on transport in the tonoplast and plasma membrane regions of the gradient. Addition of 0.3 μM valinomycin to the vesicles from the tonoplast region of the gradient prevented the buildup of a ΔpH if added prior to ATP, and caused the ΔpH to collapse if added after the ATP (not shown). Valinomycin did not collapse the ΔpH in the plasma membrane region of the gradient. In order to emphasize the activity in the plasma membrane region of the gradient, proton transport was assayed with 100 mM KNO_3 and 1.0 μM valinomycin (Fig. 2B). A single peak of activity was revealed, at a density of 1.16 $g \cdot cm^{-3}$. The activity was partially inhibited by 300 μM vanadate. The data in Figure 2, A and B, are for separate gradients, so an exact comparison of the total activities cannot be made. The gradient shown in Figure 2A was also assayed for sterol glucosyl transferase activity, which is reported to be enriched in the plasma membrane (16). There was a broad peak of activity at 1.14 to 1.17 $g \cdot cm^{-3}$ as well as large amounts of activity extending through the less dense regions of the gradient (Fig. 2C).

The effect of temperature on the proton transport activity of the gradient fractions was assessed (Fig. 3). When the fractions were assayed at 24°C (Fig. 3A) the activity in the tonoplast region of the gradient, at 1.09 to 1.15 $g \cdot cm^{-3}$, was inhibited by 50 mM KNO_3 and the activity in the plasma membrane region of the gradient, at 1.15 to 1.18 $g \cdot cm^{-3}$, was not, as in Figure 2A. When transport was assayed at 10°C (Fig. 3B) the activity in the tonoplast region of the gradient apparently was no longer inhibited by KNO_3, since similar initial rates were measured in the presence of KNO_3 and KCl, as in Figure 1 at 8°C. There was little measureable activity in the plasma membrane region of the gradient at 10°C (Fig. 3B) only because of the combination of low rates and low temperatures; activity could be measured at 10°C if the membranes were concentrated on a step gradient (not shown).

The distribution of ATPase and other enzyme activities was determined, and compared with that of the proton-transport activities (Fig. 3). There was a peak of Ca^{2+}-phosphatase (12) at the top of the gradient, a large shoulder of Ca^{2+}-stimulated ATP hydrolysis in the central portion of the gradient, and large amounts of Mg^{2+}-ATPase throughout the gradient (Fig. 3C). Large amounts of Ca^{2+}-stimulated phosphatase were also found in the 100,000*g* supernatant, and it is possible that the Ca^{2+}-phosphatase at the top of the gradient is a soluble enzyme that adhered to the membranes during isolation (12). A peak of NO_3^--inhibited ATPase coincided with the peak of NO_3^--inhibited proton transport in the tonoplast region of the gradient and a peak of vanadate-inhibited ATPase coincided with the peak of nitrate-insensitive transport in the plasma membrane region of the gradient (Fig. 3D). There was also a small peak of vanadate-inhibited ATPase that was always observed at the top of the gradients, even in the presence of ammonium molybdate (at 1.06 $g \cdot cm^{-3}$ in Fig. 3D). Therefore, it was not analogous to the vanadate-inhibited phosphatase described for corn roots (15). However, it was removed when the gradient fractions were washed with 150 mM KCl, as shown previously (12). The main peak of NADPH Cyt *c* reductase, at 1.07 to 1.09 $g \cdot cm^{-3}$ (Fig. 3E) was clearly separated from the other activities, indicating a

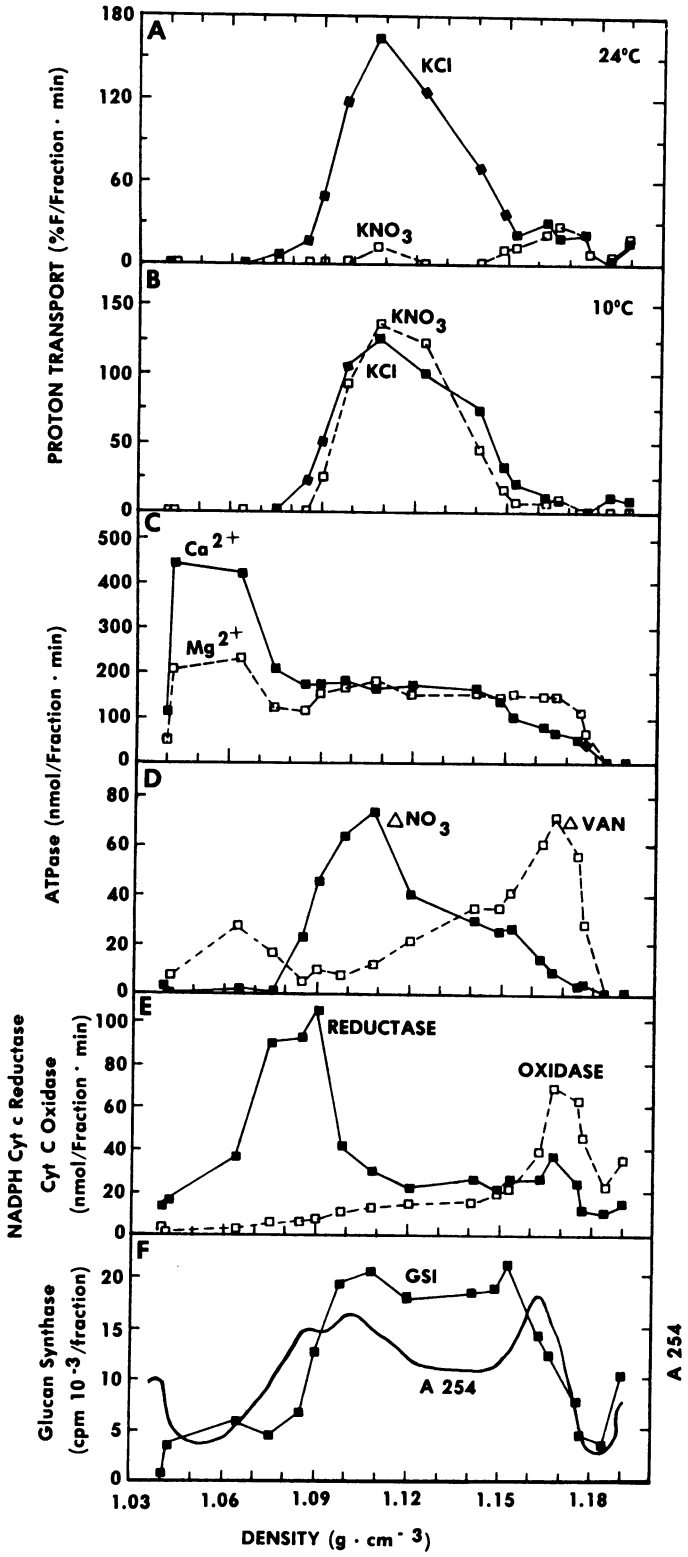

FIG. 3. Distribution of enzyme activities in a continuous sucrose gradient. A, Proton transport assayed at 24°C with 50 mM KCl (■) or 50 mM KNO_3 (□). B, Proton transport assayed at 10°C with 50 mM KCl (■) or 50 mM KNO_3 (□). C, ATPase activity assayed at 24°C with 100 μM ammonium molybdate, 1 mM NaN_3, 0.02% Triton X-100, 50 mM KCl, 1 mM Tris ATP, and 1 mM $MgSO_4$ (□) or 1 mM $CaCl_2$ (■). D, Nitrate-inhibited ATPase activity, calculated as the difference in activity assayed with 50 mM KNO_3 or 50 mM KCl (■); vanadate-inhibited ATPase, calculated as the difference in activity assayed with or without 100 μM sodium vanadate (□). Other additions as in C. E, NADPH Cyt *c* reductase (■) and Cyt *c* oxidase (□). F, Glucan synthase I (■), and A_{254} (——). The membranes were prepared from 16 g fresh weight of roots grown in 0.1 mM $CaSO_4$ at 8°C.

Table I. *Distribution of Enzyme Activities in a Preparative Step Gradient*

Membranes were prepared from roots grown in 0.1 mM $CaSO_4$ at 22°C. Activities were assayed at 24°C.

Assay	Fraction[a]		
	A	B	C
	specific activities		
NADH Cyt c[b] reductase	590	120	100
Cyt c[b] oxidase	10	210	110
Proton transport[c]			
+ 50 mM KCl	130	890	140
+ 50 mM KNO_3	0	110	106
ATPase[b,d]			
+ 1 mM Ca^{2+}	633	267	150
+ 1 mM Mg^{2+}	417	500	800
ATPase[b,d]			
KCl washed membranes[e]			
+ 1 mM Ca^{2+}	67	133	83
+ 1 mM Mg^{2+}	83	300	433

[a] Fraction A was collected from the sample/22% interface, fraction B from the 22%/30% interface, and fraction C from the 30%/40% interface. [b] nmol·min^{-1}·mg^{-1}. [c] % ΔF/F·mg^{-1} min^{-1}. [d] Assayed with 50 mM KCl. [e] Membranes washed with 150 mM KCl, as described in "Materials and Methods."

separation of ER membranes from the tonoplast ATPase activity. Additional NADPH Cyt *c* reductase activity was found throughout the gradient. The peak of Cyt *c* oxidase, a marker for mitochondrial membranes, coincided with the plasma membrane ATPase, along with a small peak of NADPH Cyt *c* reductase, at 1.16 to 1.17 g·cm^{-3} (Fig. 3E). Glucan synthase I activity, which is frequently used as a marker for Golgi membranes, was broadly distributed in the gradient. The activity in Figure 3F ranged from 1.09 to 1.16 g·cm^{-3}, with two peaks, one at 1.11 g·cm^{-3} and one at 1.15 g·cm^{-3}. The distribution of glucan synthase I was more variable between experiments than the other enzyme activities, but there was always a peak near 1.12 g·cm^{-3}, and in all cases the glucan synthase activity overlapped that of the nitrate-inhibited ATPase. IDPase was not a suitable marker for the Golgi membranes because large amounts of nonlatent IDPase coincided with the distribution of the Ca^{2+}-phosphatase (not shown). No glucan synthase II activity could be detected (not shown). The distribution of PPi-dependent proton transport (8, 28, 32) resembled that of the nitrate-inhibited, ATP-dependent proton transport (not shown).

Preparative Step Gradients. Sucrose step gradients were designed to separate the two peaks of proton transport activity, in order to facilitate additional characterization of the activities. Attempts to separate markers for Golgi membranes from plasma membrane and tonoplast markers by additional gradient steps were not successful, so it was decided to use the simplest step gradient that would resolve the two peaks of transport activity. A three-step gradient of 22, 30, and 40% (w/w) sucrose was used. The distribution of marker enzymes in the step gradient fractions was similar to that which one would predict from the distribution of activities in the continuous gradients (Table I). Fraction A was the interface between the sample and 22% sucrose, and it contained the majority of the NADH Cyt *c* reductase activity, as well as the soluble Ca^{2+}-phosphatase activity that could be removed by a wash with 150 mM KCl (12). Fraction B was collected

from the 22 to 30% interface and it contained the majority of the proton transport activity sensitive to KNO_3 at 24°C. Fraction C was collected from the 30 to 40% interface and it contained a small amount of proton transport activity, of which 24% was inhibited by KNO_3. Fraction C contained little Ca^{2+}-ATPase, and a large proportion of the Mg^{2+}-ATPase activity. The distribution of Cyt *c* oxidase was variable, and sometimes it was greater in the center of the gradient, as in Table I, but sometimes it was greater at the dense end of the gradient, as in Figure 3.

The ATPase activities of fractions A, B, and C were characterized with respect to the effects of KCl, KNO_3, and vanadate (Tables II and III). The results of two typical experiments are shown. The fractions in experiment 1 were collected from the step gradient interfaces and assayed, whereas the fractions in experiment 2 were washed with 150 mM KCl and then assayed. The assays included 1 mM Na^+ azide to inhibit the mitochondrial F_1-ATPase and 100 μM ammonium molybdate which was reported to inhibit some vanadate-sensitive phosphatases (15). A pH of 7.5 was used to optimize conditions for the tonoplast ATPase (Table II) and pH 6.5 to optimize conditions for the plasma membrane ATPase (Table III) (31). After the KCl wash, NO_3^- inhibited 55% of the ATPase of fraction B (Table II) and vanadate inhibited 25% of the ATPase of fraction C (Table III).

Table II. *Distribution of Nitrate-Inhibited ATPase in a Preparative Step Gradient*

Membranes from 40 g fresh wt of barley seedlings grown at 22°C in 0.1 mM $CaSO_4$. Assays were done at 24°C with 1 mM NaN_3, 100 μM ammonium molybdate, 0.25 M sucrose, and 50 mM KNO_3 or 50 mM KCl in 5 mM Pipes-KOH (pH 7.5). Fractions A, B, C as in Table I. Experiment 1: Total protein in fraction A was 0.6 mg, in B, 0.7 mg, and C, 0.5 mg. Experiment 2: Total protein in A was 0.9 mg, B, 1.2 mg, C, 1.0 mg. The KCl wash is described in "Materials and Methods." Numbers are means ± SD for three replicates.

Additions	ATPase Activity		
	Fraction A	Fraction B	Fraction C
	nmol Pi/mg·min		
Experiment 1: No KCl Wash			
KCl	280 ± 32	347 ± 7	365 ± 12
KNO_3	202 ± 17	168 ± 5	340 ± 28
Inhibition or stimulation	−26%	−52%	−7%
Experiment 2: KCl Wash			
KCl	125 ± 8	285 ± 8	268 ± 18
KNO_3	60 ± 10	127 ± 6	303 ± 18
Inhibition or stimulation	−52%	−55%	+13%

Table III. *Distribution of Vanadate-Inhibited ATPase in a Preparative Step Gradient*

The membrane fractions are the same as in Table II. Assays were done with 1 mM NaN_3, 100 μm ammonium molybdate, 0.25 M sucrose, 1 mM $MgSO_4$, 1 mM ATP, and 50 mM KNO_3 in 5 mM Pipes-KOH (pH 6.5) with 100 μM sodium vanadate where indicated. Fractions A, B, C as in Table I. Numbers are means ± SD for three replicates.

Additions	ATPase Activity		
	Fraction A	Fraction B	Fraction C
	nmol Pi/mg·min		
Experiment 1: No KCl Wash			
None	410 ± 18	248 ± 7	505 ± 18
+ Vanadate	436 ± 28	271 ± 12	403 ± 38
Inhibition or stimulation	+6%	+9%	−20%
Experiment 2: KCl Wash			
None	103 ± 2	200 ± 3	375 ± 7
+ Vanadate	123 ± 2	187 ± 7	281 ± 25
Inhibition or stimulation	+19%	−7%	−25%

The KCl washes removed a large amount of the contaminating Ca^{2+}-phosphatase activity, particularly from fraction A (*cf.* experiments 1 and 2 in Tables II and III), but a large background of ATPase activity that was not affected by nitrate, vanadate, azide, or molydate remained in all fractions. A partial test of substrate specificity of the background ATPase was made, as part of the search for an enzyme activity to use for a Golgi membrane marker. Triton X-100 was included in the assays to reveal latent activity and the assays were carried out at pH 7.5 in the presence or absence of 1 mM $MnCl_2$. There was high activity in the absence of divalent cations, and rates for ADP and IDP were similar and not stimulated by Mn^{2+} (not shown).

In summary, step gradients separated three fractions enriched respectively in ER (fraction A), a NO_3^--inhibited ATPase that was probably the tonoplast ATPase (fraction B), and a vanadate-inhibited ATPase that was probably the plasma membrane ATPase (fraction C). The enrichment of the plasma membrane ATPase in fraction C can be improved by collecting the membranes from a 34/40% interface, instead of from the 30/40% interface used in this paper (data not shown). Further proof of the origins of the ATPases was obtained by reacting immunoblots of barley membrane fractions with antibodies to the corn tonoplast and plasma membrane ATPases. Antibodies to the 70 and 60 kD protein of the tonoplast ATPase from corn coleoptiles reacted strongly with a respective 70 and 60 kD protein that were enriched in fraction B of the barley membranes (22). Also, antibodies prepared against a 100 kD protein isolated from a band on an SDS gel of a partially purified plasma membrane ATPase from corn roots (14) were found to react strongly with a 100 kD protein in fraction C of the barley root membranes (unpublished results, in cooperation with W Hurkman, USDA, Albany, CA).

Effect of Temperature and NO_3^- on Proton Transport and ATP Hydrolysis by Fraction B Vesicles. A detailed characterization of the effect of temperature on the H^+-ATPases of fraction B was performed in order to determine whether the NO_3^--sensitive and NO_3^--insensitive proton transport in fraction B was due to a single enzyme or two separate enzymes. Proton transport was assayed at different temperatures in the presence of 50 mM KCl or 50 mM KNO_3. Examples from a representative experiment are shown in Figure 4. The assays were performed in duplicate, and the replicate traces were nearly identical if superimposed and compared. Triton X-100 was added to dissipate the pH gradient; it caused the fluorescence to return to a slightly higher intensity than the initial value, possibly because it decreased the turbidity of the sample. There was no pre-existing ΔpH and addition of 3 mM ammonium chloride caused the fluorescence to return to the original level (not shown).

The initial rate of proton transport at 3°C was greater with 50 mM KNO_3 than with 50 mM KCl (Fig. 4). In the presence of KNO_3 there was a rapid initial rate of proton transport, followed by subsequent decay of the pH gradient. Fluorescence returned to the original intensity if the assay was continued for a long enough time (not shown). For the examples shown in Figure 4, reversal of the slope began by 2 min at 3°C and by 30 s at 21°C. In some experiments, reversal of the slope was delayed as long as 5 min at 3°C. When membranes from fraction C were assayed in the same manner, they maintained a pH gradient in the presence of 50 mM KNO_3 for over 30 min (not shown).

One possible explanation for the effect of temperature on the sensitivity of the ATPase to nitrate was that the extent to which ATP hydrolysis was inhibited by KNO_3 decreased as a function of temperature. Therefore, the effect of KNO_3 on ATP hydrolysis was tested at a range of temperatures. Results from a representative experiment are shown in Table IV. Approximately 49% of the activity was inhibited by 50 mM KNO_3 at 24°C, similar to the results in Table II, and approximately 38% of the ATPase

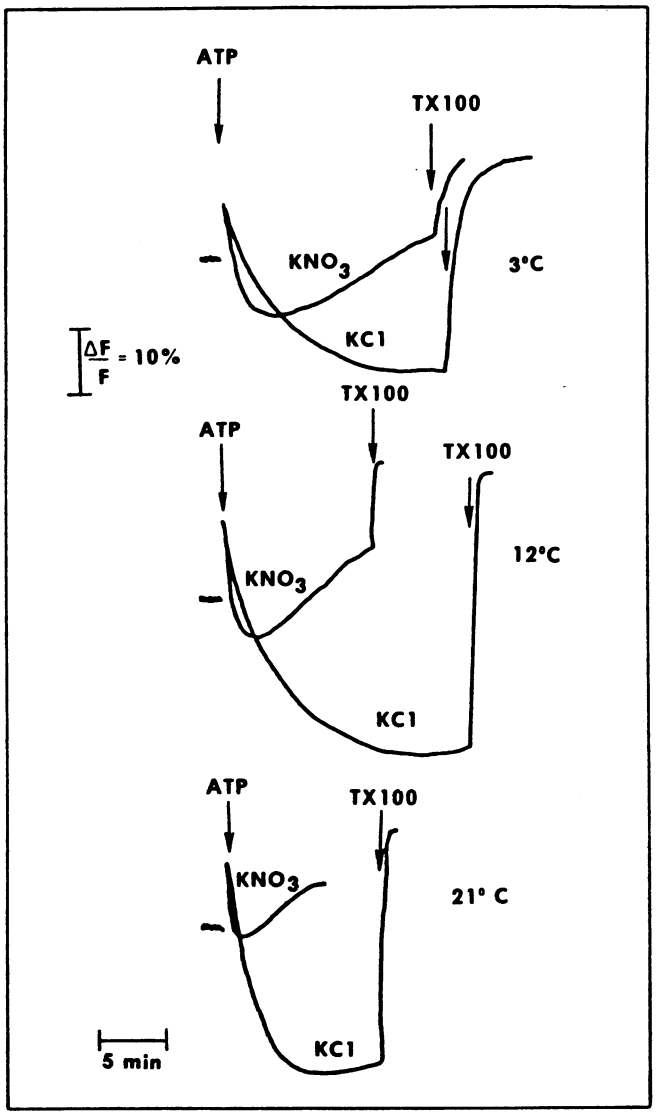

FIG. 4. Response of acridine orange fluorescence to addition of ATP. Fraction B vesicles (Table I) (39 μg protein per assay) were assayed at the indicated temperatures with 50 mM KNO_3 or 50 mM KCl. Triton X-100 was added to give a concentration of 0.02% at second arrow. The membranes were from roots grown in full nutrients at 8°C.

Table IV. *Effect of Temperature and Salt on Rate of ATP Hydrolysis*

Fraction B membranes were assayed with 50 mM KCl or 50 mM KNO_3 at the indicated temperatures. Pi was assayed as in Figure 5 and the rates were determined from slopes that were calculated by linear regression analysis ($r > 0.9935$ for all slopes). Membranes were from roots grown in full nutrients, including nitrate, at 8°C.

Temperature	Additions	ATPase	Inhibition
°C		*nmol Pi/mg·min*	%
12	KCl	299	
	KNO_3	184	38
24	KCl	494	
	KNO_3	254	49
36	KCl	1472	
	KNO_3	834	43

activity was inhibited at 12°C. The differences in rate were not significant, and when nitrate inhibition was calculated for a complete range of temperatures from 0 to 44°C the percent inhibition was not correlated with the assay temperature (not shown).

An alternative explanation for the biphasic response of transport to nitrate (Fig. 4) was that lowering the assay temperature caused the lag in NO_3^--inhibition of the ATPase to increase by slowing the rate at which NO_3^- gained access to the site of inhibition. Therefore, the effect of NO_3^- on the time course for ATP hydrolysis was examined (Fig. 5). At 12°C there was a lag of 2 min before inhibition by nitrate could be detected. Similar measurements were made at 24 and at 36°C (not shown) but any lag at the higher temperatures was too short to measure by the technique that was used.

The vesicles were exposed to KNO_3 for less than 1 min prior to addition of ATP for the assays of Figures 3 to 5. The effect of longer incubation in KNO_3 prior to addition of ATP was tested (Fig. 6). Preincubation with 50 mM KNO_3 for 5 to 10 min at 14°C prior to addition of ATP significantly decreased the maximum quench attained. Preincubation with 50 mM KCl only slightly decreased the initial rates and maximum quench.

Proton transport and ATP hydrolysis were assayed as a function of the concentration of KCl or KNO_3. The K_i for inhibition by NO_3^- was between 5 and 10 mM, if the ATPase activity that was not inhibited by 50 mM KNO_3 was considered to be a nonspecific background activity (not shown). Both ATP hydrolysis and proton transport were significantly inhibited by 5 mM KNO_3 in the presence of 50 mM KCl at 8, 24, and 36°C (not shown).

DISCUSSION

Two peaks of ATP-dependent proton transport were separated on continuous sucrose gradients of barley root membranes (Figs. 2–3). A large peak of activity at 1.08 to 1.13 $g \cdot cm^{-3}$ had characteristics in common with the tonoplast-type ATPase (3, 5, 9, 20, 21, 26, 31) and a smaller peak of activity at 1.14 to 1.18 $g \cdot cm^{-3}$ had characteristics in common with the plasma membrane ATPase (10, 15, 31). Glucan synthase I, a marker enzyme for Golgi membranes, overlapped both peaks of transport activity. The transport activities of the two peaks were examined in detail because of the scarcity of reliable criteria to differentiate between the proton translocating ATPase of tonoplast, Golgi membranes, and plasma membranes.

The proton translocating ATPase of the plasma membrane fraction from barley roots was only partially inhibited by a

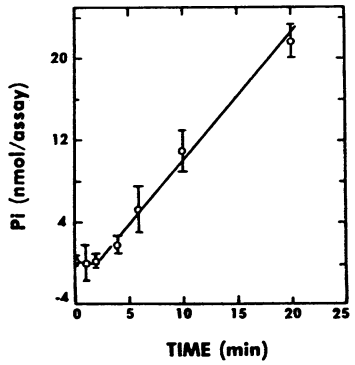

FIG. 5. Nitrate inhibition of ATP hydrolysis as a function of time at 12°C. Fraction B vesicles were assayed with 50 mM KCl or 50 mM KNO_3 and the difference in Pi released at each time point was calculated (NO_3^--inhibited ATPase). All data points were collected in triplicate, and the bar indicates SD. Membranes (10 μg protein per assay) were from roots grown at 8°C in 0.1 mM $CaSO_4$.

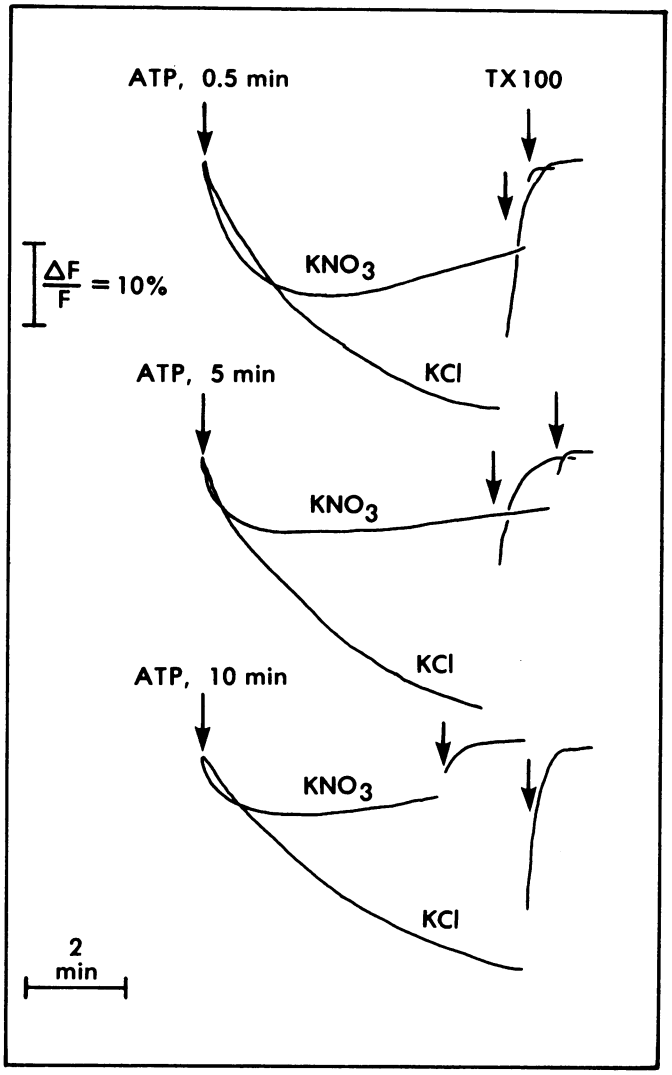

FIG. 6. Effect of preincubation in 50 mM KNO_3 on the time course of fluorescence quench at 14°C. Fraction B vesicles were assayed as in Figure 4. Membranes (20 μg protein per assay) were added to a reaction mix containing 50 mM KCl or KNO_3 as indicated and incubated at 14°C for 0.5, 5, or 10 min, as indicated, before addition of ATP. The second arrow indicates the addition of Triton X-100 to a final concentration of 0.02%. The membranes were from roots grown in full nutrients at 22°C.

relatively high concentration of vanadate (Fig. 2). Similar results were reported for a plasma membrane fraction from corn roots (10). The gradient fractions that were used for Figures 2 and 3 of this paper contained EDTA (12), which will complex with vanadate (6), and the assay conditions, such as pH and concentration of Mg^{2+}, may not have been optimal for obtaining complete inhibition by vanadate (6). However, the extent of inhibition of the ATPase by vanadate was not greatly improved when EDTA was removed by a KCl wash (Table III). The amount of vanadate-inhibited ATPase was similar to the amount of nitrate-inhibited ATPase (Fig. 3D), yet the amount of ATP-dependent proton transport in the plasma membrane region was much less than in the tonoplast region of the gradient (Fig. 3A). It is likely that only a small proportion of the membranes in the plasma membrane fraction consisted of sealed, inside-out vesicles capable of maintaining a ΔpH, whereas the majority of the plasma membrane ATPase was on unsealed vesicles. There probably were also sealed, right-side-out vesicles with no measureable ATPase activity, since that is the principal form of plasma membrane vesicle that was recovered by a 2-phase procedure (17).

A proton-translocating ATPase on Golgi membranes may also be present in the plasma membrane and/or the tonoplast-enriched fractions. Unfortunately, there are few criteria to identify the Golgi membrane ATPase. Ali and Akawaza (1) reported that the Golgi membrane ATPase was not inhibited by KNO_3, but Chanson and Taiz (7) reported that it was partially inhibited by KNO_3. If the H^+-ATPase of barley membranes that was insensitive to vanadate or nitrate was the Golgi membrane ATPase, then the small peak of transport activity in the plasma membrane region of the gradient (Fig. 2B) may have been a composite of the activities of the Golgi and plasma membrane ATPases. This cannot be determined without a more specific inhibitor to the Golgi membrane ATPase.

Valinomycin caused the ΔpH to collapse in the tonoplast region of the gradient (not shown) but it did not collapse the ΔpH in the plasma membrane region of the gradient (Fig. 2B). This may be a useful criterion to distinguish tonoplast from Golgi and plasma membranes in corn and barley. For example, a concentration of 1 μM valinomycin stimulated proton transport by the Golgi membrane ATPase of corn coleoptiles (7) and the plasma membrane ATPase of corn roots (10), but it partially inhibited transport by the tonoplast ATPase (7). The different effects of valinomycin could be caused by differences in the lipid composition of the membranes and corresponding differences in the partition coefficients for the valinomycin-K^+ and valinomycin-H^+ complex. In contrast to the findings for corn and barley, valinomycin did not collapse the ΔpH of tonoplast vesicles from red beet (3).

Since antibodies to the 70-kD and 60-kD subunits of the corn tonoplast ATPase gave a strong cross-reaction with similar proteins in the barley fraction B, collected at 22 to 30% sucrose, it is likely that the majority of the H^+-ATPase in that region of the gradient is analagous to the tonoplast H^+-ATPase of corn (22). However, Golgi and tonoplast membranes have been reported to have a similar density on sucrose gradients (1, 7, 8, 19) and fraction B contained a peak of glucan synthase I. Therefore, it is possible that fraction B contained Golgi membrane ATPase. However, it is not likely that the biphasic time course for proton transport that was observed in the presence of NO_3^- (Fig. 4) was caused by the activity of two different enzymes. The results in Figure 4 are not easily accounted for by combining the activity of a nitrate-insensitive and a nitrate-inhibited enzyme, for instance, since complete inhibition was obtained by assaying with 100 mM KNO_3 plus 1.0 μM valinomycin (Fig. 2B), and since 50 mM KNO_3 eventually caused the entire ΔpH to collapse.

The two-phase time course that was observed in response to 50 mM KNO_3 can be explained in terms of the activity of a single enzyme. The initial stimulation of transport by NO_3^- (Figs. 4 and 6) was most likely due to the ability of NO_3^- to relieve the membrane potential (4, 18). In some experiments, such as those shown in Figure 4, higher initial rates of proton transport were obtained with NO_3^- than with Cl^- (Fig. 4), which may indicate that NO_3^- was more effective than Cl^- in relieving the membrane potential (25, 33). It is interesting that the rate of efflux of anions from vacuoles of barley leaves followed the order $NO_3^- > Cl^- > Pi$, which is the order of anion chaotropicity (23). Anion channels are apparently not required for this effect, since Cl^- and NO_3^- were used as permeant anions to stimulate proton transport by a purified H^+-ATPase that was reconstituted into liposomes (25).

There are several possible explanations for the subsequent collapse of the pH gradient. The simplest explanation is that nitrate directly inhibited the ATPase. There are several reports that NO_3^- inhibited ATP hydrolysis with a K_i of 5 to 10 mM (27, 31 and references therein) and similar results were found for the barley ATPase. Inhibition by NO_3^- was independent of its effect

on membrane potential, since it inhibited the ATPase in the presence of ionophores (3) and it inhibited the detergent solubilized ATPase (21). Churchill and Sze (9) proposed that NO_3^- binds to an anion-sensitive site that regulates the catalytic and vectorial activity of the tonoplast H^+-ATPase. They suggested that the enzyme assumes an active configuration when Cl^- binds to the site and an inactive configuration when NO_3^- binds to the site. The simplest hypothesis to explain the delay before NO_3^- inhibits the barley ATPase is that the anion binding site is on the cytoplasmic side of the ATPase and a conformational change in the protein is required for NO_3^- to bind. The conformational change might be sufficiently slow at temperatures below 20°C that a lag is observed before NO_3^- inhibits the ATPase. The site for vanadate-inhibition of the plasma membrane ATPase is apparently on the cytoplasmic side of the enzyme, yet Bowman and Slayman (6) reported a 5 min lag before vanadate inhibited the *Neurospora* plasma membrane ATPase. A similar biphasic time course was observed with DCCD in the barley tonoplast vesicles (not shown), and for corn tonoplast vesicles (Ref. 7, Fig. 8A).

An alternative hypothesis is that the binding site for NO_3^- is on the vacuolar lumen side of the membrane, so that NO_3^- does not inhibit the enzyme until a sufficiently high intravesicular concentration of NO_3^- develops. There would be a lag before the enzyme was inhibited at low temperatures if lowering the assay temperature lowered the rate of transport of NO_3^- into the vesicles. However, the enzyme would rarely be active *in vivo* if the inhibitory site were on the vacuolar lumen side, since the concentration of NO_3^- in the vacuole can be as high as 40 mM (23).

An additional explanation for the efflux of protons from the vesicles may be that NO_3^- dissipates the ΔpH via a NO_3^-/H^+ symport (6). Lew and Spanswick (18), and Blumwald and Poole (4) also demonstrated that, under certain circumstances, NO_3^- stimulated proton transport by the H^+-ATPase of tonoplast vesicles. Both groups performed a type of experiment that was similar, but not identical, to that shown in Figure 4. They also measured the formation and dissipation of pH gradients by observing the decrease and increase, respectively, of acridine orange fluorescence. The Mg^{2+}-ATP was added to vesicles in the absence of K^+ salts, so that a large membrane potential but only a small ΔpH was formed, and KCl or KNO_3 were added later. Additions of either salt caused an immediate influx of protons into the vesicles followed by a steady state ΔpH if KCl was added, or subsequent dissipation of the pH gradient if KNO_3 was added. Blumwald and Poole (4) proposed that the dissipation of the pH gradient was not caused by inhibition of the ATPase but by activation of a NO_3^-/H^+ symport. They proposed that such a symport may have the physiological function of carrying NO_3^- but not Cl^- out of the vacuole. They arrived at the conclusion that a symport was involved because they used 5 mM KNO_3 to observe the effect, and 5 mM KNO_3 did not inhibit ATP hydrolysis. Lew and Spanswick (18) observed a similar biphasic time course for proton transport in the presence of 50 mM KNO_3, but this concentration clearly inhibited ATP hydrolysis. I performed the same experiment, by adding 50 mM KNO_3 to membranes from barley and tomato after the addition of MgATP. The results (not shown) were similar to those shown in Figure 4 and inhibitory concentrations of KNO_3 stimulated proton influx before causing the ΔpH to collapse. It has been reported that NO_3^- is stored in the vacuoles of barley roots during the night and released to the shoots during the day (29). Release of NO_3^- from the vacuole by a regulated symport is an attractive hypothesis. However, the biphasic time course that was observed *in vitro* can be explained by a delay in inhibition of the tonoplast ATPase by NO_3^- and is insufficient evidence for the action of a NO_3^-/H^+ symport.

The only other evidence for a NO_3^-/H^+ symport was that KNO_3 partially inhibited the buildup of a ΔpH by the tonoplast pyrophosphatase although PPi hydrolysis was not inhibited by KNO_3 (28, 32). However, KNO_3 stimulated proton transport by the pyrophosphatase from corn coleoptiles (8). In order to prove the existence of a NO_3^-/H^+ symport it will be necessary to use pH jumps to demonstrate that addition of KNO_3 can drive H^+ efflux and that a ΔpH will drive efflux of NO_3^-.

The relationship between the effect of NO_3^- on the tonoplast ATPase *in vitro* and *in vivo* is not yet clear. A question of particular importance is whether NO_3^- actually inhibits the ATPase *in vivo*. The barley ATPase was partially inhibited *in vitro* by only 5 mM KNO_3, even in the presence of 50 mM KCl, which may be similar to cytoplasmic concentrations of Cl^- and NO_3^- (23). The soil temperature which barley roots experience *in vivo* is often lower than 20°C, but this would not protect the ATPase from inhibition by NO_3^-, since low assay temperatures only delayed the inhibitory effects of nitrate for a few min. If the anion-sensitive site is on the cytoplasmic side of the tonoplast ATPase, where ATP hydrolysis occurs, the cytoplasmic concentration of NO_3^- may be in a critical range capable of modulating the activity of the ATPase. However, the strong inhibition produced by exposure of the site of ATP hydrolysis to 50 mM NO_3^- in the *in vitro* assays may represent a nonphysiological condition.

Many of the experiments in this paper utilized membranes from roots grown at 8 or 10°C. One object of the original experiments was to determine if there was a low temperature optimum for transport by barley membranes, since the roots grew well at 8°C. The tonoplast ATPase did function well at low assay temperatures (Figs. 1, 3B, 4), and the ability to assay the barley membranes at low temperatures, and obtain relatively high rates of transport was useful for observing the temperature dependence of the response to NO_3^-.

The results in this paper can be accounted for by a model in which NO_3^- inhibits the tonoplast ATPase by binding to an anion-binding site on the cytoplasmic side of the ATPase. Lowering the assay temperature may lower the rate of the conformational change required for NO_3^- to bind and inhibit the ATPase. If NO_3^- penetrated the membrane vesicles more rapidly than it was able to bind to the inhibitory site on the ATPase, one would observe an initial stimulation of proton influx, followed by inhibition of the ATPase and subsequent dissipation of the pH gradient, just as is shown in Figure 4.

The results demonstrate that caution must be used if inhibition by NO_3^- is used to distinguish the tonoplast H^+-ATPase from other ATPases, because observations of proton transport for a short time, as in Figure 1, or without preincubation in NO_3^-, as in Figure 6, might not reliably show the inhibition.

Acknowledgments—Thanks to W. Hurkman for many useful discussions, and to K. Summers for technical assistance.

LITERATURE CITED

1. Ali MS, T Akazawa 1986 Association of H^+-translocating ATPase in the Golgi membrane system from suspension-cultured cells of Sycamore (*Acer pseudoplatanus* L.) Plant Physiol 81: 222–227
2. Ames BN 1966 Assay of inorganic phosphate, total phosphate and phosphatase. Methods Enzymol 8: 115–118
3. Bennett AB, SD O'Neill, RM Spanswick 1984 H^+-ATPase activity from storage tissue of *Beta vulgaris*. Plant Physiol 74: 538–544
4. Blumwald E, RJ Poole 1985 Nitrate storage and retrieval in *Beta vulgaris*: effects of nitrate and chloride on proton gradients in tonoplast vesicles. Proc Natl Acad Sci USA 82: 3683–3687
5. Boller T, A Wiemken 1986 Dynamics of vacuolar compartmentation. Annu Rev Plant Physiol 37: 137–164
6. Bowman BJ, CW Slayman 1979 The effects of vanadate on the plasma membrane ATPase of *Neurospora crassa*. J Biol Chem 254: 2928–2934
7. Chanson A, L Taiz 1985 Evidence for an ATP-dependent proton pump on the Golgi of corn coleoptiles. Plant Physiol 78: 232–240
8. Chanson A, J Fichmann, D Spear, L Taiz 1985 Pyrophosphate-driven proton transport by microsomal membranes of corn coleoptiles. Plant Physiol 79:

159–164
9. Churchill KA, H Sze 1984 Anion-sensitive, H^+-pumping ATPase of oat roots. Plant Physiol 76: 490–497
10. De Michelis MI, RM Spanswick 1986 H^+-pumping driven by the vanadate-sensitive ATPase in membrane vesicles from corn roots. Plant Physiol 81: 542–547
11. DuPont FM, AB Bennett, RM Spanswick 1982 Localization of a proton-translocating ATPase on sucrose gradients. Plant Physiol 70: 1115–1119
12. DuPont FM, WJ Hurkman 1985 Separation of the Mg^{2+}-ATPases from the Ca^{2+}-phosphatase activity of microsomal membranes prepared from barley roots. Plant Physiol 77: 857–862
13. Epstein E, JD Norlyn 1977 Seawater-based crop production: a feasibility study. Science 197: 249–251
14. Gallagher SR 1985 Purification and electrophoretic analysis of the plant plasma membrane ATPase. PhD Dissertation. University of California, Riverside
15. Gallagher SR, RT Leonard 1982 Effect of vanadate, molybdate and azide on membrane-associated ATPase and soluble phosphatase activities of corn roots. Plant Physiol 70: 1335–1340
16. Hartmann-Bouillon M-A, P Benveniste 1978 Sterol biosynthetic capability of purified membrane fractions from maize coleoptiles. Phytochem 17: 1037–1042
17. Korner RLE, P Kjellbom, C Larsson, JM Moller 1985 Surface properties of right side-out plasma membrane vesicles isolated from barley roots and leaves. Plant Physiol 79: 72–79
18. Lew RR, RM Spanswick 1985 Characterization of anion effects on the nitrate-sensitive ATP-dependent proton pumping activity of soybean (*Glyine max* L.) seedling root microsomes. Plant Physiol 77: 352–357
19. Mandala S, IJ Mettler, L Taiz 1982 Localization of the proton pump of corn coleoptile microsomal membranes by density gradient centrifugation. Plant Physiol 70: 1743–1747
20. Mandala S, L Taiz 1985 Proton transport in isolated vacuoles from corn coleoptiles. Plant Physiol 78: 104–109
21. Mandala S, L Taiz 1985 Partial purification of a tonoplast ATPase from corn coleoptiles. Plant Physiol 78: 327–333
22. Mandala S, L Taiz 1986 Characterization of the subunit structure of the maize tonoplast ATPase. Immunologic and inhibitory binding studies. J Biol Chem 261: 12850–12855
23. Martinoia E, MJ Schramm, G Kaiser, WM Kaiser, U Heber 1986 Transport of anions in isolated barley vacuoles. Plant Physiol 80: 895–901
24. Niemietz C, J Willenbrink 1985 The function of tonoplast ATPase in intact vacuoles of red beet is governed by direct and indirect ion effects. Planta 166: 545–549
25. Perlin DS, K Kasamo, RJ Brooker, CW Slayman 1984 Electrogenic H^+-translocation by the plasma membrane ATPase of *Neurospora*. J Biol Chem 259: 7884–7892
26. Poole RJ, DP Briskin, Z Kratky, RM Johnstone 1984 Density gradient localization of plasma membrane and tonoplast from storage tissue of growing and dormant red beet. Plant Physiol 74: 549–556
27. Randall SK, Y Wang, H Sze 1985 Purification and characterization of the soluble F_1-ATPase of oat root mitochondria. Plant Physiol 79: 957–962
28. Rea PP, RJ Poole 1985 Proton-translocating inorganic pyrophosphatase in red beet (*Beta vulgaris* L.) tonoplast vesicles. Plant Physiol 77: 46–52
29. Rufty TW, DW Israel, WJ Volk 1984 Assimilation of $^{15}NO_3$ taken up by plants in the light and in the dark. Plant Physiol 76: 769–775
30. Sanui H 1974 Measurement of inorganic orthophosphate in biological materials: extraction properties of butyl acetate. Anal Biochem 60: 489–504
31. Sze H 1985 H^+-translocating ATPases: advances using membrane vesicles. Annu Rev Plant Physiol 36: 175–208
32. Wang Y, RA Leigh, KH Kaestner, H Sze 1986 Electrogenic H^+-pumping pyrophosphatase in tonoplast vesicles of oat roots. Plant Physiol 81: 497–502
33. Wolosin JM, JG Forte 1983 Kinetic properties of the KCl transport at the secreting apical membrane of the oxyntic cell. J Membr Biol 71: 195–207